



AMERICAN JOURNAL OF  
**BIOSCIENCE AND BIOINFORMATICS (AJBB)**

ISSN: 2995-0481 (Online)

**VOLUME 3 ISSUE 1 (2024)**



PUBLISHED BY  
**E-PALLI PUBLISHERS, DELAWARE, USA**

## Evaluating the Impact of Seed Nano-Priming with Green-Synthesized Copper Oxide Nanoparticles Using *Mimosa pigra* Leaf Extract on the Germination and Seedling Growth of Tomato (*Solanum lycopersicum*)

H. K. S. Madusanka<sup>1\*</sup>, A. G. B. Aruggoda<sup>1</sup>, J. A. S. Chaturika<sup>2</sup>, S. R. Weerakoon<sup>3</sup>

### Article Information

**Received:** October 30, 2023

**Accepted:** December 03, 2023

**Published:** December 24, 2023

### Keywords

*Copper Oxide Nanoparticles, Green-Synthesized Nanoparticles, Mimosa Pigra Leaf Extract, Seed Nano-Priming, Tomato (Solanum lycopersicum) Germination*

### ABSTRACT

This study explores the impact of seed nano-priming with green-synthesized copper oxide nanoparticles (CuO NPs) using *Mimosa pigra* leaf extract on the germination and seedling growth of tomato (*Solanum lycopersicum*). CuO NPs were synthesized through a plant-mediated green synthesis approach, where phytochemicals in *M. pigra* extract reduced Cu<sup>2+</sup> ions and stabilized the nanoparticles. The resulting nanoparticles were characterized using UV-vis spectroscopy and SEM, revealing a surface plasmon resonance (SPR) peak at 224 nm and a nanoscale morphology with an average size of 108 nm. XRD analysis confirmed a crystalline monoclinic structure, with an average crystallite size of 30.68 nm. FTIR spectra showed characteristic Cu-O bond vibrations and plant-related functional groups, confirming successful nanoparticle synthesis. Seed germination experiments evaluated the effects of CuO NPs across a concentration gradient (0–1000 ppm). Results demonstrated a biphasic effect on germination and seedling growth. Low concentrations (5–100 ppm) enhanced germination percentages and growth metrics, while higher concentrations (≥500 ppm) inhibited these parameters. The 50 ppm treatment exhibited the highest germination rate, whereas 1000 ppm significantly suppressed seed germination and seedling growth. Statistical analysis indicated significant differences in root and shoot lengths across treatments, with oxidative stress and genotoxicity attributed to higher CuO NP concentrations as key inhibitory factors. These findings highlight the dual role of CuO NPs, emphasizing the potential of green-synthesized nanoparticles as bio-enhancers at optimal concentrations, while cautioning against their phytotoxic effects at elevated levels. This research underscores the need for further studies to optimize nanoparticle applications in agriculture and mitigate environmental risks.

### INTRODUCTION

Nanoparticles are very small particles with dimensions ranging between 1 and 100 nanometers in size and have a higher surface area-to-volume ratio. Therefore, nanoparticles exhibit properties different from those of their bulk form. Synthesis of nanoparticles is categorized into three main protocols: physical, chemical, and biological. This classification is based on the reducing agent or electrical source involved in the synthesis process (Shende *et al.*, 2015). In the physical method, the source of electrons is a physical source such as an electrical current. In the chemical method, the electron source is a chemical solvent, and in the biological method, the electron source is an organism or a biomolecule (Khaldari *et al.*, 2021). Growing interest in biological methods utilizes natural resources such as bacteria, fungi, algae, and plant extracts as reducing and capping agents to synthesize nanoparticles (Sabouri *et al.*, 2020). Studies have been conducted and have successfully identified the properties of nanoparticles as antioxidant, anticoagulant, antibacterial, and antimicrobial agents (Zahra Sabouri *et al.*, 2022). The application of nanoparticles in agriculture is a trending and promising development for a better future. In agriculture, nanoparticles can act as fertilizers, fungicides, bactericides, and insecticides (Feigl,

2023). Once nanoparticles uptake into plants, they get translocated and affect the growth and development by both promoting or retarding the physiological processes (Li *et al.*, 2015, Murali *et al.*, 2022). Plants can take up nanoparticles from the entire plant surface such as roots, shoots, etc. (Wang *et al.*, 2023). They further described that nanoparticles move from roots through primary root pores, penetrate the root cell wall, and are taken up from leaves through the periderm pores and stomata. After being absorbed, these nanoparticles are conveyed through the plant via both symplastic and apoplastic routes, facilitating their movement within the organism (Feigl, 2023). Plants showed varied responses to nanoparticles based on their specific species, owing to differences in their physiological characteristics and the growth medium (Dev *et al.*, 2017).

The research involved the green synthesis of CuO NPs by utilizing *M. pigra* plant extract. The synthesized nanoparticles underwent a thorough characterization. Subsequently, the study explored the potential influence of these CuO NPs on both seed germination and seedling growth of tomato. Different concentrations of the nanoparticle suspension were employed to assess their effects, aiming to identify any consequential impacts during the process.

<sup>1</sup> Department of Agricultural and Plantation Engineering, The Open University of Sri Lanka, Nawala, Nugegoda, Sri Lanka

<sup>2</sup> Department of Urban Bio-resources, University of Sri Jayawardanapura, Ganagodawila, Nugegoda, Sri Lanka

<sup>3</sup> Department of Botany, The Open University of Sri Lanka, Nawala, Nugegoda, Sri Lanka

\* Corresponding author's e-mail: [hksma@ou.ac.lk](mailto:hksma@ou.ac.lk)

## LITERATURE REVIEW

Copper is an abundant metal in the Earth's crust, with an availability of 60 mg/kg of Cu in the lithosphere, and soils typically contain 2-50 mg/kg (Alloway, 2014). CuO NPs have various impacts on plants, both positive and negative, on growth and development. Studies conducted on CuO NPs have revealed that the effects include higher growth and production, greater stress tolerance, better defence mechanisms against pathogens, and improved nutrient uptake and utilization (Faraz *et al.*, 2023). Still, a higher concentration of Cu causes oxidative stress, negative effects on the uptake of other elements, reduced photosynthetic pigment levels, and impairment of cellular components in plants (Shabbir *et al.*, 2020). In a study conducted by Zhang *et al.* (2019), it was concluded that plants exposed to higher concentrations of Cu exhibit various toxic symptoms, including root and shoot growth retardation, and in some cases, the death of the plant (Zhang *et al.*, 2019). The mechanism behind growth retardation involves the generation of higher levels of Reactive Oxygen Species (ROS), leading to oxidative stress, subsequent cytotoxicity, and damage to DNA (Naz *et al.*, 2020). CuO NPs toxicity could also be caused by the Fenton reaction, where Cu ions convert hydrogen peroxide into hydroxyl radicals, resulting in damage to nearby macromolecules (Chung *et al.*, 2019). Alternatively, a lack of copper can lead to diverse abnormalities in plants, including the distortion of young leaves, necrosis, bending of stems, compromised vegetative growth, and diminished quality of grains (Siddiqi & Husen, 2020). Seed priming is a simple and effective hydration strategy to promote seed germination. During this process, seeds undergo physiological changes that result in improved and increased pre-germinative metabolic processes (Dawood, 2018). Seed nano-priming involves the use of suspensions or Nano formulations in which specific nanoparticles can be taken up by the seeds (Acharya *et al.*, 2019). Once the seeds are introduced to the nanoparticle suspension, the nanoparticles are taken up from the solution by the seeds, and the majority of the taken-up nanoparticles reside in the seed coat (Gabriel *et al.*, 2020). The high concentration of nanoparticles in the seed coat could act as a barrier to pathogens, functioning as fungicides or bactericides (Gross *et al.*, 2020). Hence, nanoparticles in the seeds can act on pathogens directly or by altering the metabolism of seeds or seedlings to enhance the innate immune system. They can also alter hormone production, thereby making the plants more resistant to diseases or abiotic stresses (Panyuta *et al.*, 2016).

The *Mimosa* genus belongs to the Fabaceae family, specifically the subfamily Mimosoideae, encompassing approximately 400 varieties of shrubs and herbs (Ahuchaogu *et al.*, 2017). A study conducted on screening the phytochemicals in *M. pigra* using methanol and water revealed the presence of flavonoids, quinones, saponins, sterols, and tannins in the leaves and (Rosado-Vallado *et al.*, 2000) tannins, phlorotannins, flavonoids, triterpenes and saponins in roots (Olusayo *et al.*, 2016).

Phytochemicals serve as both reducing and capping agents in the green synthesis of nanoparticles. These compounds play a crucial part in stabilizing the nanoparticles, preventing agglomeration, and controlling both size and morphology in the synthesis of metal oxide nanoparticles (Hosseinzadeh *et al.*, 2023).

## MATERIALS AND METHODS

### Materials

*Mimosa pigra* fresh plant leaves were collected from Uhana, Ampara, Sri Lanka. Extra pure AR cupric sulfate ( $\text{CuSO}_4 \cdot 5\text{H}_2\text{O}$ , minimum purity 99.5 %) was purchased from Sisco Research Laboratories Pvt. Ltd. Sodium hydroxide pellets (NaOH, minimum purity 98 %) was purchased from Loba Chemie Pvt. Ltd. Tomato seeds (*Solanum lycopersicum*) of the "Thilina" variety were acquired from a certified seed producer with registration number SA/CMB/00023, minimum germination rate of 75 % and an expiration date of 17 November 2024. Freshly prepared double-distilled water (DDW) was used for the experiment.

### Preparation of the Mimosa Pigra Extract

The leaves of *Mimosa pigra* were washed in running tap water for five minutes and soaked in DDW thrice. Subsequently, the leaves were dehydrated at 42 °C for 24 hours. The leaf debris was separated, and the remaining pinnules were isolated. The collected pinnules were ground followed by sieving to eliminate larger particles. Six grams of dry powder were added to 100 ml of DDW and heated at 60 °C for one hour while continuously stirred by a magnetic stirrer. The leaf debris was separated from the extraction by filtering thrice using Whatman No. 1 filter paper. The filtrate was subsequently used for synthesis of nanoparticles.

### Synthesis of CuO NPs

A 0.01 M  $\text{CuSO}_4$  solution was prepared and stirred for 30 minutes at room temperature. The freshly prepared plant extract filtrate was mixed with the precursor salt in a 1:9 ratio, respectively. While the mixture was under constant stirring, the pH was raised to 10 by incrementally adding 1 M sodium hydroxide. The reaction mixture was stirred for two hours, then left undisturbed for 24 hours to facilitate the synthesis of CuO NPs. After the incubation time, the colloidal solution was centrifuged at 6000 rpm for 10 minutes to obtain a pellet, which was then purified by washing with DDW thrice. The final sediment was hot air-dried for 12 hours at 80 °C, and the dried CuO NPs were crushed by a mortar and pestle, and the fine powder was stored for future use.

### CuO NPs Characterization

The prepared CuO NPs were synthesized by bioreduction of copper ions using a plant extract, which was confirmed by visually observing the color change. UV-visible spectroscopy analysis was performed on the nanoparticle suspension made with DDW to confirm the

successful synthesis of CuO NPs in the resolution of 1 within the range of 190 nm to 450 nm using a quartz cuvette. To determine the morphology of the synthesized nanoparticles, a Scanning Electron Microscope (SEM) analysis was conducted. The SEM pictures were analyzed, and particle size was measured using Image J software (Schneider *et al.*, 2012). X-ray diffraction (XRD) techniques were used to classify the green synthesised CuO NPs nanoparticles and the presence of phase and crystal structure in CuO NPs was determined. The IR spectra spectrum given in cm<sup>-1</sup> were recorded on ATR method by Fourier Transform Infrared Spectroscopy (FTIR).

### Seed Preparation

The tomato seeds underwent a cleaning process, starting with a 5-minute washing under running tap water, followed by immersing in a 5 % (v/v) detergent solution for an additional 5 minutes. Subsequently, the seeds were disinfected using 70 % (v/v) ethanol solution for 1 minute. Additional disinfection was carried out by immersing the seeds in 1.5 % (v/v) NaOCl solution for 10 minutes. Finally, the seeds were rinsed three times using DDW, each time seeds were kept submerged for 5 minutes, to remove any remaining disinfectant.

### Germination Experimental Design

Different concentrations (5, 10, 50, 100, 500, and 1000 ppm) of CuO NPs solutions were prepared using DDW, subjected to sonication for one hour at a temperature of 40 °C. Tomato seeds were then immersed for 4 hours in the respective concentration solutions of CuO NPs. Sterilized tissue paper was positioned in each petri dish, and subsequently, 2 ml of CuO NPs suspension was promptly poured after thorough agitation of each treatment concentration. Ten pre-soaked seeds were placed in each petri dish, covered, sealed with parafilm, and allowed to germinate *in vitro* in an incubator at room temperature (25 °C) for seven days. On the 3rd day, 1 ml of DDW was added to each petri dish. The experimental design was a completely randomized design (CRD) with five replicates, and observations were conducted

daily for seven consecutive days to count the number of germinated seeds. On the 8th day, root length, shoot length, and fresh weight were measured.

### Germination Parameters

The final germination percentage (FGP) is considered as the average number of seeds that germinate during the set time period and is calculated according to the equation mentioned below (01).

$$FGP \% = (\text{number of germinated seeds} / \text{number of incubated seeds}) \times 100 \quad (01)$$

On the 8th day, the seedlings were collected, and their biometric data, comprising shoot length (mm), root length (mm), and fresh weight of seedlings (mg), were measured and then averaged. The Vigor Index was determined using the provided equation (02) from Krushangi Maisuria and Patel (2009).

$$\text{Vigor Index} = \{ \text{Root length (mm)} + \text{Shoot length (mm)} \} \times \text{Seed germination \%} \quad (02)$$

### Data Analysis

The data were analyzed to determine the significance of each treatment compared to the control group (5, 10, 50, 100, 500, and 1000 ppm). Statistical analysis was performed on all experiment parameters using a completely randomized design and the one-way ANOVA test conducted by R statistical software. A p-value less than 0.0001 was considered statistically significant compared to the control group. Subsequently, Duncan's Multiple Range Test (DMRT) and Dunnett's test were employed to assess the least significant difference between pairs of means. The graphs were generated using R statistical software.

## RESULTS AND DISCUSSION

### Mechanism of CuO NPs Synthesis

The formation of metallic nanoparticles through plant extract-mediated green synthesis follows a bottom-up approach and can be categorized into three phases: The activation phase, the Growth phase, and the Termination phase (Redhi, 2018).

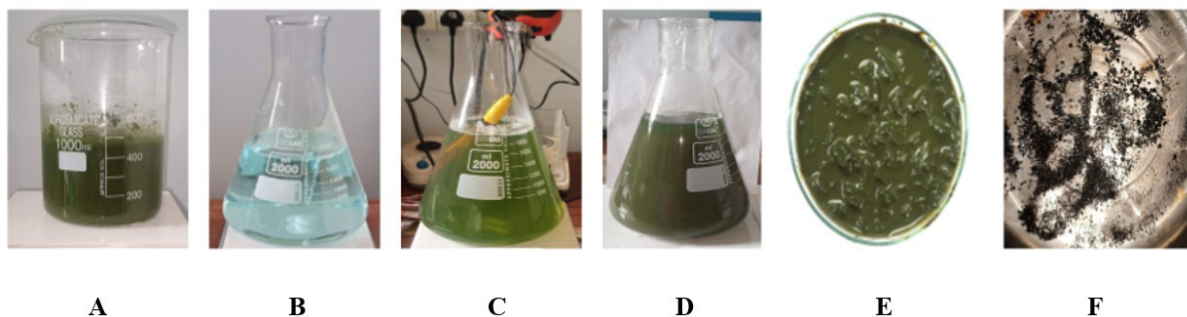


**Figure 1:** (A) plant extract, (B) precursor salt, (C) mixture of plant extract and precursor salt, (D) mixture of plant extract and precursor salt after adjusting pH to 10, (E) extracted nanoparticles before drying, (F) nanoparticle after drying.

In the activation phase, metal salt solution undergoes reduction into metal ions via phytochemical constituents, followed by nucleation of metal atoms leading to the

formation of particles with an increased size range compared to the atomic level. The synthesis concludes with the termination phase, where the capping of active

molecules onto the surface of the metals provides steric hindrance, limiting particle aggregation and ensuring a stable morphology and size in the nano-range, ultimately leading to the formation of stable metal nanoparticles (Singh *et al.* 2021). Bioactive molecules such as flavonoids, alkaloids, saponins, steroids, terpenoids, and tannins play a crucial role in reducing metal ions to metals and stabilizing them in the colloidal size range (Kuppusamy *et al.*, 2016). Mimosa leaf extract, rich in diverse phytochemicals, effectively reduces Cu<sup>2+</sup> ions (formed upon dissolving CuSO<sub>4</sub> in water) and acts as a capping agent for the nanoparticles. The Cu<sup>2+</sup> ions undergo reduction to copper atoms, initiating the growth phase where atoms aggregate and form nanoparticles (Alhalili, 2022). Upon the drop-by-drop addition of 1 M sodium hydroxide to the mixture, the solution undergoes a spontaneous color change from green to dark green to brown as illustrated in Figure 01, indicating the formation of CuO-NPs (Amin *et al.*, 2021).

The synthesis of nanoparticle morphology is influenced by various parameters, including plant material, extraction method, phytochemical content, pH of the mixture, reaction temperature, reactant concentration, reaction time, and product recovery (Singh *et al.*, 2021). The type of plant material (root, leaves, fruit) and various factors such as climate, age of the plant, and geographical location significantly impact the composition of phytochemicals in the plant (Banu, 2015). Different extraction methods

and various solvents can result in extracting distinct phytochemicals from the plant material (Altemimi *et al.*, 2017). Changes in pH impact the alteration of charges in plant metabolites, thereby influencing the reduction and chelation of metal ions during the process (Vijayaraghavan & Ashokkumar, 2017).

Temperature plays a significant role in determining nanoparticle size, shape, and yield. Typically, elevated temperatures are observed to enhance the nucleation rate, consequently promoting the production of crystalline nanoparticles (Lade & Shanware, 2020). The concentration of the precursor salt and the phytochemical concentration of the plant extract has a significant impact on the formation of nanoparticles. As the concentration increases, the synthesis of nanoparticles also increases (Seifpour *et al.*, 2020). The reaction time of the mixture affects the synthesis of nanoparticles, as various plant phytochemicals influence the activation, growth, and termination phases differently for each type of nanoparticle. The final production of stabilized nanoparticles varies in time depending on the plant extract used, the method employed, and the concentration applied (Ahmad *et al.*, 2016). The final product recovery yields crystals for nanoparticle synthesis, but processes such as calcination or drying may induce changes in particle size due to agglomeration.

#### Characterization of CuO NPs.

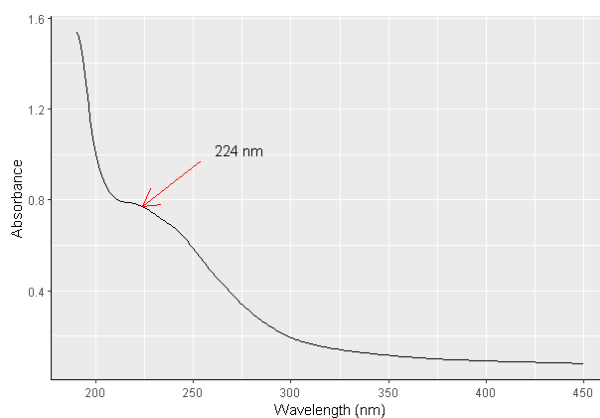


Figure 2: UV-vis spectroscopy analysis of CuO NPs

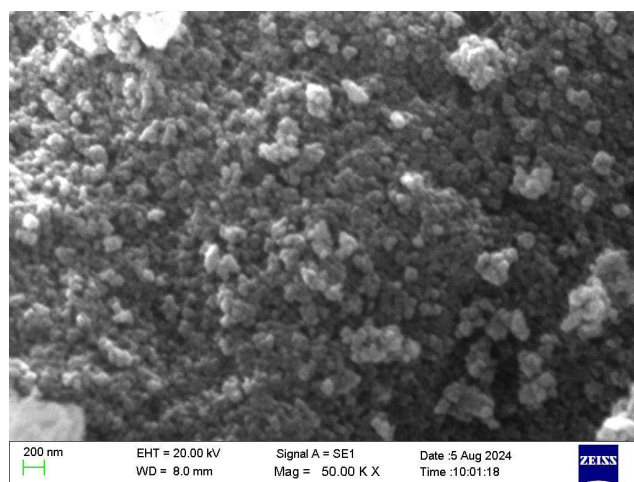


Figure 3: SEM images of CuO NPs at a scale of 200 nm

Surface plasmon resonance (SPR) within the range of 190nm to 450 nm was observed, with peak absorbance at 224 nm, confirming the green synthesis of nanoparticles as illustrated in Figure 02. Similar results were obtained through the green synthesis of CuO NPs using *Pimpinella anisum* seed extract, with peak UV-vis absorbance observed in the range of 250 nm to 300 nm (Elamin & Taha, 2023). Rangasamy *et al.*, in 2023, studied the green synthesis of CuO NPs using *Tecoma stans*, having a similar absorption peak at 296 nm. Further, studies done by Amaliyah *et al.*, in 2020 by green synthesising CuO NPs from *Piper retrofractum* as a bio reductant and capping agent, revealed that the UV Vis spectrophotometer readings of SPR peak at 234 - 255 nm. These results are in par with the results we received from the present study. The SEM images presented in Figure 03 revealed the diverse shapes and sizes of CuO NPs. These nanoparticles

exhibit a range of shapes and sizes within the nanoscale dimension, with an average diameter of approximately 108 nm. Additionally, they demonstrate a tendency to aggregate and exist in from oval to circular shapes. CuO NPs were synthesized through green synthesis methods using orange peel extract or mint leaves extract, with copper sulfate serving as the precursor salt, and the synthesis process did not involve calcination but instead entailed oven drying at 45 °C for 24 hours. The resulting CuO NPs were found to be in the nanometer range, approximately 150 nm in size (Mahmoud *et al.*, 2021). Copper oxide nanoparticles were synthesized via green synthesis using *Antigonon leptopus* leaf extract and copper sulfate, followed by air drying in an oven at 80 °C without undergoing calcination. The resulting nanoparticles exhibited a size range between 110 to 280 nm (Sravanthi *et al.*, 2016).

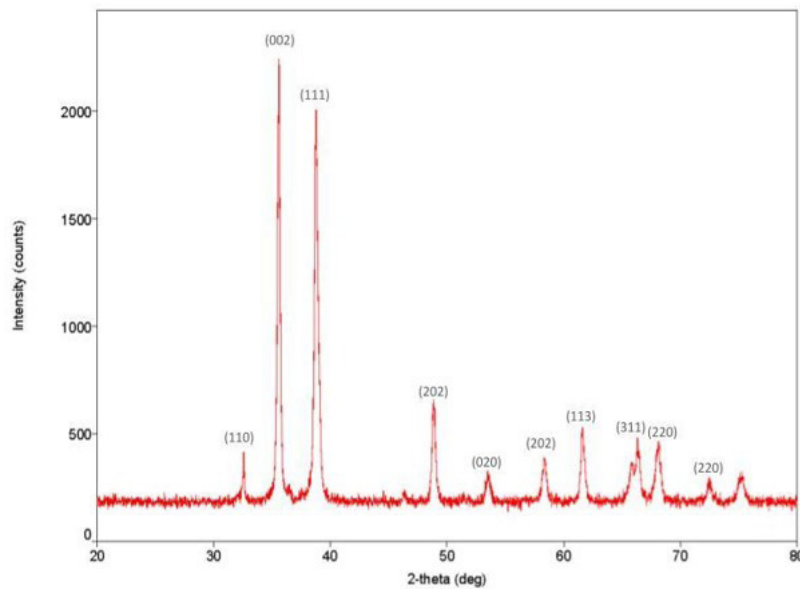


Figure 4: XRD pattern for CuO NPs

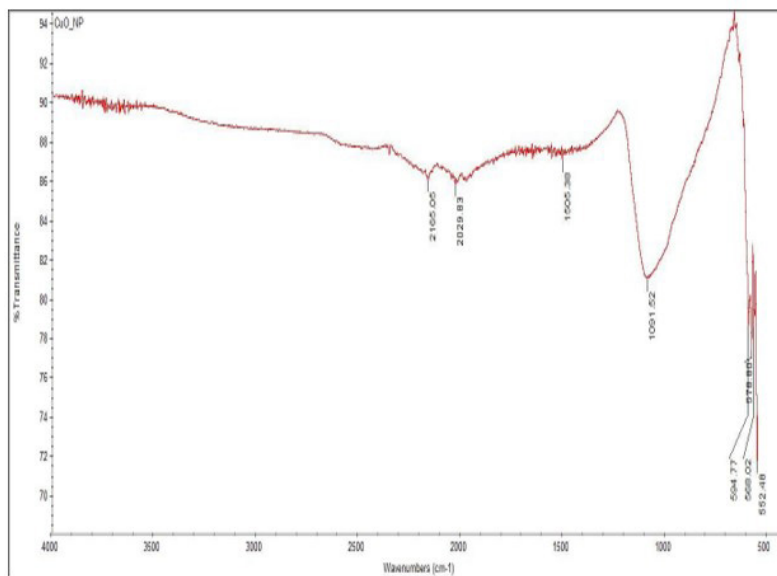


Figure 5: FTIR spectra of CuO NPs

The X-ray diffraction pattern of green-synthesized CuO NPs is illustrated in Figure 04. This pattern was investigated at 40 kV and 30 mA using a K-beta filter (CuK $\alpha$  radiation,  $\lambda = 0.15406$  nm). XRD data revealed the crystalline structure of the synthesized CuO NPs, with peak positions at 32.59°, 35.6°, 36.49°, 38.73°, 46.25°, 48.83°, 53.49°, 58.36°, 61.61°, 65.80°, 66.33°, 68.16°, and 72.48°, indexed as (110), (002), (002), (111), (202), (202), (020), (202), (113), (311), (311), (220), and (220) planes, respectively. These results match the standard CuO diffraction data from the Joint Committee on Powder Diffraction Standards (JCPDS 45-0937), indicating the crystalline monoclinic structure. The average crystalline size of the synthesized NPs was calculated as 30.68 nm using the Debye-Scherrer formula (Ganesh Kumar *et al.*, 2016).

$D = K\lambda/\beta\cos\theta$  (3)  
 Where D denotes the crystallite size of copper oxide nanoparticles,  $\lambda$  is the wavelength of the X-ray source (0.15406 nm) used in XRD,  $\beta$  is the full width at half maximum (FWHM) of the diffraction peak, K is the Scherrer constant, which ranges from 0.9 to 1, and  $\theta$  is the

Bragg angle. The difference between the SEM value and the crystallite size calculated from the XRD data could be due to the aggregation of nanoparticles and surface amorphous materials on the NPs.

The synthesized CuO NPs were characterized using FTIR spectroscopy, and the results are illustrated in Figure 05. The spectrum shows strong absorption bands at 595.45, 584.08, 576.09, and 560.42  $\text{cm}^{-1}$ , which can be attributed to Cu-O bond vibrations, confirming the synthesis of CuO nanoparticles (Alhalili, 2022). The presence of O-H stretching frequencies is indicated at 3851.29 and 3646.98  $\text{cm}^{-1}$ , while the C $\equiv$ C (alkyne) stretching or C $\equiv$ N (nitrile) groups are observed at 2165.48  $\text{cm}^{-1}$ . The frequency peak at 1505.59  $\text{cm}^{-1}$  (C=C stretching vibrations) could be attributed to aromatic compounds, possibly from plant phenols, and the frequency peak at 1093.12  $\text{cm}^{-1}$  (C-O stretching) could be due to the presence of alcohols, ethers, or esters from the plant extract. Similar results have also been reported in previous work where CuO nanoparticles were synthesized using different leaf extracts (Černík & Thekkae Padil, 2013; Shkir, 2022).

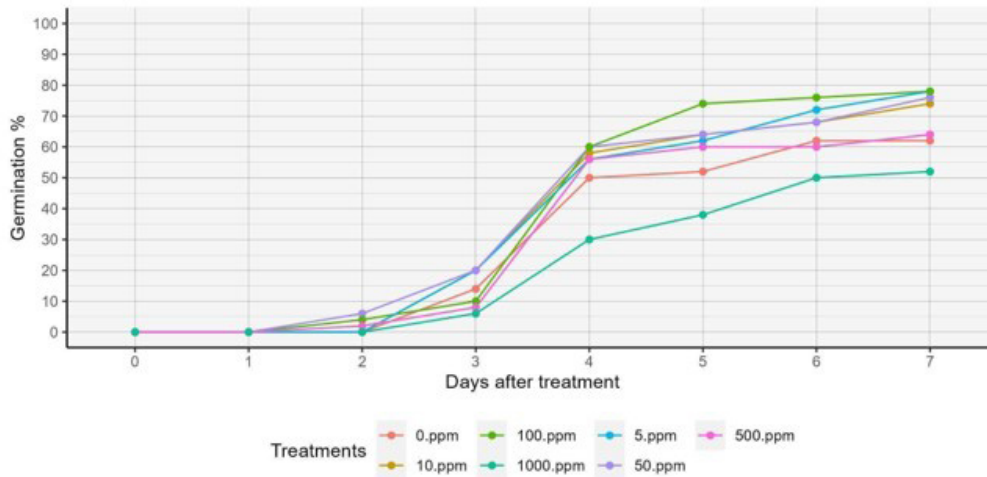


Figure 6: The cumulative daily germination percentage of tomato seeds

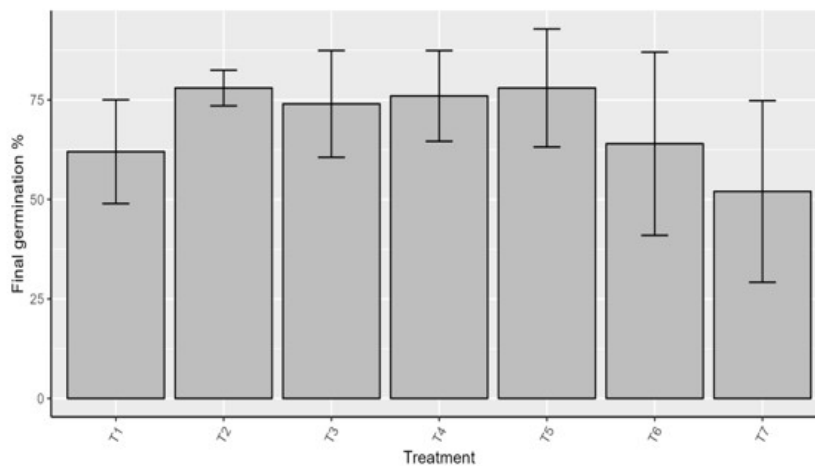


Figure 7: Effect of different concentrations of CuO NPs on the final germination percentage of tomato seeds after 7 days of incubation. Bars illustrate  $\pm$  standard error. T1 (0 ppm), T2 (5 ppm), T3 (10 ppm), T4 (50 ppm), T5 (100 ppm), T6 (500 ppm), T7 (1000 ppm)

### Effect of CuO NPs on Germination

Seeds treated with different concentrations of CuO NPs were allowed to germinate, and the daily cumulative germination percentage was calculated and illustrated in Figure 04. The germination of tomato seeds commenced on day 2, with the highest percentage of germinated seeds observed in treatment added with 50 ppm treatment, while the lowest germination percentage was observed in the 1000 ppm treatment. On day 5, the highest germination percentage was observed in the 100 ppm treatment, while the lowest was observed in the 1000 ppm treatment. Additionally, all other treatments exhibited higher germination percentages compared to the control treatment (0 ppm).

From Figure 06, it is evident that the germination percentage of the 1000 ppm treatment consistently remained lower than that of the other treatments. Treatments with concentrations of 5 ppm, 10 ppm, 50 ppm, and 100 ppm exhibited a similar trend in germination. In 500-ppm concentrated treatment, the germination percentage increased until the 5th day, after which there was little to no further increase in germination percentage. As depicted in Figure 07, the final germination percentage was highest in the 5 ppm treatment ( $78 \pm 4.47\%$ ) and the 100 ppm treatment ( $78 \pm 14.83\%$ ). Conversely, the minimum final germination was observed in the treatment with 1000 ppm treatment ( $52 \pm 22.80\%$ ), while the control treatment resulted with the germination percentage of  $62 \pm 13.03\%$ . The statistical analysis using one-way ANOVA indicated that there is no significant difference among the treatments, with a p-value less than 0.0001 (F value = 1.10,  $P > F = 0.10$ ).

The study conducted on germination of *Hordeum vulgare* L. var. Ardhaoui seeds treated with copper oxide nanoparticles revealed consistent results. The highest final and cumulative germination percentage was observed at a

concentration of 100 mg/L, while the lowest was recorded at a concentration of 2000 mg/L (Kadri *et al.*, 2022). The researchers concluded that low concentrations of CuO NPs led to enhanced seed germination parameters. However, the present study revealed the inhibitory effects of concentrations exceeding 500 ppm on seed germination.

As per the investigations of Khodakovskaya *et al.* (2012) Copper nanoparticles have been observed to come into contact with seed coats, penetrate the seeds, and enhance seed germination and seedling growth in plants. The elevated rates of seed germination could be attributed to the photo-generation of ROS such as hydroxide anions and superoxide, which facilitate the re-activation of aged seeds (Zheng *et al.*, 2005). Increased concentrations of CuO nanoparticles can induce oxidative stress and harm plant cells, ultimately leading to diminished growth and yield (Feigl, 2023). Genotoxicity could be a cause of low germination of seeds at higher concentrations of CuONPs. Nanoparticle-induced genotoxicity can be categorized into two mechanisms: direct or indirect genotoxicity. Direct genotoxicity occurs when nanoparticles pass through the cell and nucleus membranes via diffusion or endocytosis and directly interact with the DNA. Indirect genotoxicity, nanoparticles interact with nuclear proteins or induce oxidative stress via ROS, thereby impairing DNA function (Karami *et al.*, 2016). The salinity of the environment surrounding the seed affects seed germination through osmotic stress (Munns, 2002), which inhibiting water absorption during the imbibition process by elevating the external osmotic potential and thereby lowering germination rate and longer germination time (Munns & Tester, 2008). Concentrations exceeding 100 ppm may contribute to poor or reduced germination percentages due to osmotic stress induced by CuO NPs.

### Effect of CuO NPs on Seedling Growth

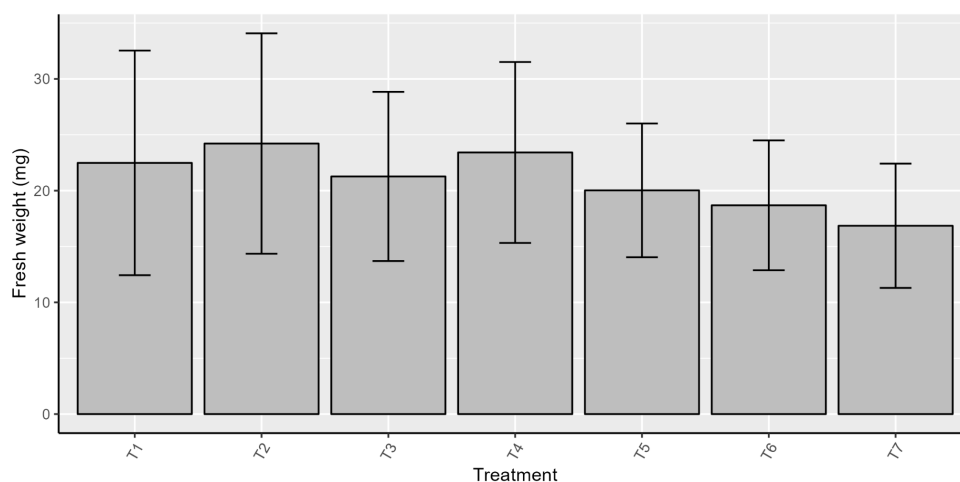


**Figure 8:** Effect on different concentrations of CuO NPs on fresh weight (mg). Results illustrated the means of population and the bar illustrates  $\pm$  standard error. T1 (0 ppm), T2 (5 ppm), T3 (10 ppm), T4 (50 ppm), T5 (100 ppm), T6 (500 ppm), T7 (1000 ppm).

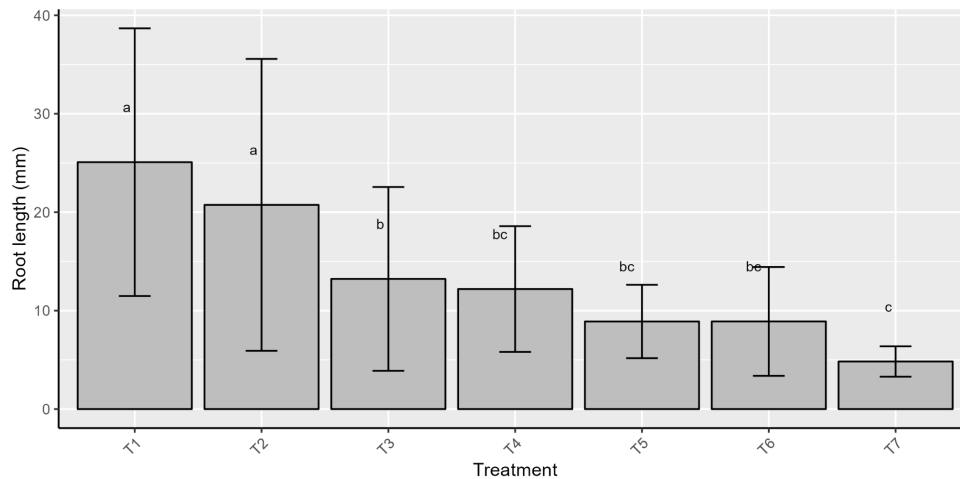


**Figure 9:** Effect on different concentrations of CuO NPs on root length (mm). Results illustrated the means of population and the bar illustrates  $\pm$  standard error. Different letters above the bars indicate significant differences at  $p < 0.0001$  per DMRT analysis. T1 (0 ppm), T2 (5 ppm), T3 (10 ppm), T4 (50 ppm), T5 (100 ppm), T6 (500 ppm), T7 (1000 ppm)

In the analysis of fresh weight of seedlings using one-way ANOVA, no significance difference was observed among the treatments, with a p-value of less than 0.0001 (F value = 3.289,  $P > F = 0.004$ ). As illustrated in Figure 08, the highest mean fresh weight was obtained from the 5-ppm treatment, measured at  $24.22 \pm 9.86$  mg, while the lowest was recorded in the 1000 ppm treatment, with the recorded value of  $16.86 \pm 5.56$  mg. The control treatment (0 ppm) resulted with a fresh weight of  $22.48 \pm 10.05$  mg. The treatments of 10 ppm, 50 ppm, 100 ppm, and 500 ppm had mean fresh weights of  $21.27 \pm 7.57$ ,  $23.41 \pm 8.10$ ,  $20.03 \pm 5.99$ , and  $18.69 \pm 5.81$  mg, respectively. Effect of ethylene on copper oxide nanoparticle-induced toxicity in rice seedlings treated with concentrations of 0, 100, 250, 450, and 600 mg/L, were studied by Azhar *et al.* (2022), resulted with a significant reduction in the fresh weight of both shoot and root weight with increasing concentration. The lowest fresh weight at 600 mg/L, while the maximum fresh weight in the treatment with 0 ppm. In another study on the effects of copper oxide nanoparticles on the growth of rice, where rice seeds were treated with concentrations of 62.5, 125, and 250 mg/L CuO NPs, it was found that these concentrations led to reductions in the weight of rice roots and leaves compared to the control. Specifically, the weight of rice roots decreased by 31.1 %, 67.2 %, and 73.5 %, respectively, while the weight of rice leaves decreased by 38.4 %, 62.7 %, and 72.8 %, respectively, compared to the control treatment (Yang *et al.*, 2020). They further described that the decrease in fresh weight was attributed to the phototoxicity of CuO NPs on rice seedlings. Similar phototoxic effects have been observed in several studies involving different plant species such as *Schoenoplectus tabernaemontani* (Zhang *et al.*, 2014), wheat (Dimkpa *et al.*, 2012), and rice (Shaw and Hossain, 2013). Further, a study conducted to investigate the effects of CuO NPs on *Triticum aestivum* L. at a concentration of 150 mg/L increase the ROS, Reactive Nitrogen Species (RNS), and

Hydrogen Sulfide (H<sub>2</sub>S) content, which contributed to the inhibition of growth (Kacziba *et al.*, 2023). Once copper enters the plant, toxicity can occur through the generation of excess ROS, leading to oxidative stress and subsequent cytotoxicity. Additionally, there is the potential for CuO NPs to cause genetic damage (Naz *et al.*, 2020). If CuO nanoparticles release Cu ions, these ions can bind to protein thiol groups, inducing conformational changes in the proteins (Feigl, 2023). Another mechanism of toxicity is through the Fenton reaction, where Cu ions catalyze the conversion of hydrogen peroxide into hydroxyl radicals, resulting in damage to nearby macromolecules (Chung *et al.*, 2019). Moreover, the effect of CuO NPs on the fresh weight of tomatoes exhibited a biphasic pattern: at low concentrations, there was an increase in fresh weight, whereas in high concentrations, fresh weight decreases when compared to the control treatment. Further studies are required to understand the underlying causes of this biphasic effect.

Root length was analyzed using one-way ANOVA, and a significant difference was observed with a confidence interval of 0.0001 (F=16.06). The Dunnett test revealed that the treatments added with 10, 50, 100, 500, and 1000 ppm exhibited significant differences when compared to the control treatment (0 ppm). DMRT separated the means of each treatment, as mentioned in Figure 09. The maximum mean root length was observed in the control group (0 ppm), with a mean root length of  $25.08 \pm 13.60$  mm, while the minimum was recorded in the treatment group of 1000 ppm, which was  $4.83 \pm 1.5434$  mm. According to the DMRT analysis, both the treatment groups 0 and 5 ppm showed no significant difference in mean root length (5 ppm recorded as  $20.74 \pm 14.83$  mm). Treatment with 10 ppm had a significant mean root length difference compared to 0 ppm and 5 ppm, recorded as  $13.22 \pm 9.34$  mm. The treatments of 50 ppm, 100 ppm, and 500 ppm showed no significant difference with each other but had a significant difference compared

to other treatments, with mean root lengths of  $12.19 \pm 6.39$ ,  $8.90 \pm 5.53$ , and  $8.90 \pm 3.73$  mm, respectively. The treatment effect demonstrates a downward trend as the concentration of CuO NPs increases, indicating a negative effect on the root length of the tomato seedlings. Consistent results were observed in the research conducted by Khaldari, Naghavi, and Motamedi, (2021), on the treatment of tomato seeds with green-synthesized nanoparticles in the range of 0, 4, 40, 400, and 4000  $\mu\text{g}/\text{mL}$ . Except for the 4  $\mu\text{g}/\text{ml}$  treatment, all other treatments showed a retardation of root growth. A similar pattern was recorded for lettuce in the same research, where concentrations over 4  $\mu\text{g}/\text{ml}$  caused retardation of root growth. The impact of nanoparticles on plants can exhibit a wide range of outcomes, influenced by various nanoparticle characteristics including their type, size, concentration, as well as chemical and physical properties. Additionally, plant-specific factors play a significant role in determining the effects observed (Shalaby *et al.*, 2016). In the study investigating the impact of excessive copper

on tomato plants, focusing on growth parameters, enzyme activities, chlorophyll, and Mineral Content, researchers confirmed a decline over time in dry mass, root length, and foliar area, correlating with increased concentrations of copper solution. Notably, copper accumulation was more pronounced in roots compared to leaves. Furthermore, the uptake of minerals was notably influenced by rising copper concentrations in the solution, with calcium (Ca), iron (Fe), and zinc (Zn) contents in leaves showing a decrease (Martins & Mourato, 2006). The diminished root length observed in tomato seedlings may stem from DNA deformation induced by the elevated accumulation of copper in the roots. As the concentration of copper increases, so does its accumulation in the roots of the seedlings, consequently leading to the inhibition of root growth. The study on 10-day lettuce seedlings exposed to Cu in the form of CuO NPs (16 nm diameter) revealed root inhibition as the concentration of CuO NPs gradually increased from 0 ppm to 798.9 ppm. Contrary to expectations, the conclusion drawn from

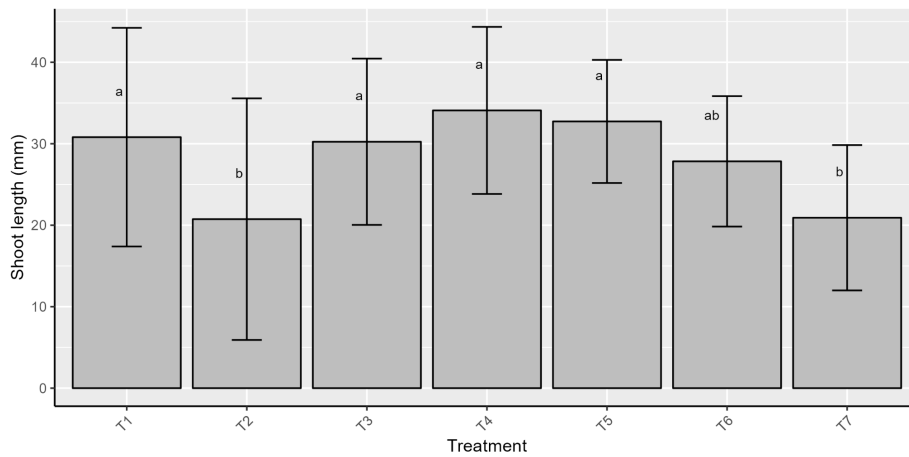


**Figure 10:** Effect on different concentrations of CuO NPs on shoot length (mm). Results illustrated the means of population and the bar illustrates  $\pm$  standard error. Different letters above the bars indicate significant differences at  $p < 0.0001$  per DMRT analysis. T1 (0 ppm), T2 (5 ppm), T3 (10 ppm), T4 (50 ppm), T5 (100 ppm), T6 (500 ppm), T7 (1000 ppm)

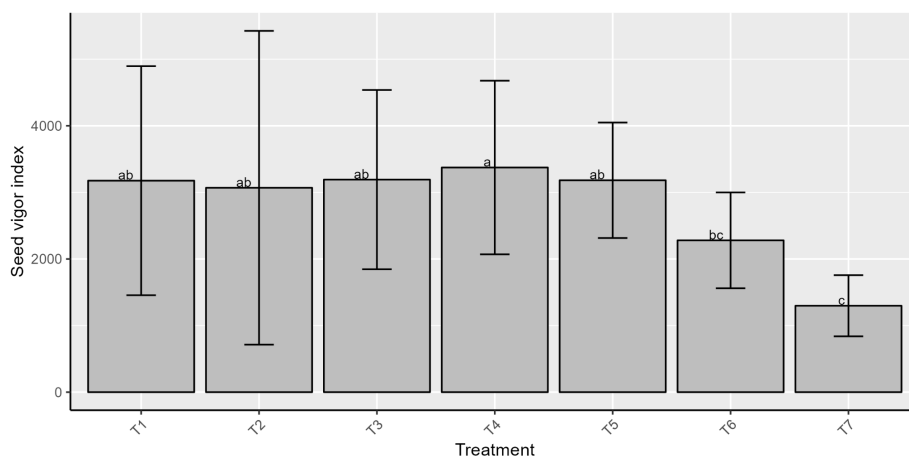


**Figure 11:** Effect on different concentrations of CuO NPs on seed vigor index. Results illustrated the means of population and the bar illustrates  $\pm$  standard error. Different letters above the bars indicate significant differences at  $p < 0.0001$  per DMRT analysis. T1 (0 ppm), T2 (5 ppm), T3 (10 ppm), T4 (50 ppm), T5 (100 ppm), T6 (500 ppm), T7 (1000 ppm)

their findings suggested that the effect on root length induced by CuO NPs may not solely be attributed to Cu<sup>2+</sup> toxicity but could be specific to the crop species under investigation (Margenot *et al.*, 2018). These studies collectively elucidate the ROS effect induced by CuO NPs on tomato seedlings, resulting in the inhibition of root length. The presence of ROS, triggered by the exposure to CuO NPs, leads to a significant reduction in root length across various concentrations. This phenomenon underscores the detrimental impact of CuO NPs on the root development of tomato seedlings, highlighting the need for further research to understand the underlying mechanisms and potential mitigation strategies.

Shoot lengths of different concentrations of CuO NPs were recorded and analyzed using one-way ANOVA, revealing a significant difference at a confidence level of 0.0001 ( $F = 7.91$ ). According to DMRT, mean differences were grouped as depicted in Figure 10. The maximum shoot lengths were observed in groups of 0, 10, 50, and 100 ppm, with mean shoot lengths of  $30.81 \pm 13.42$ ,  $30.24 \pm 10.20$ ,  $34.09 \pm 10.25$ , and  $32.74 \pm 7.56$  mm, respectively. The lowest shoot lengths were obtained in the groups of 5 and 1000 ppm, recorded as  $20.74 \pm 14.83$  and  $20.92 \pm 8.92$  mm, respectively. Additionally, the group treated with 500 ppm showed no significant difference from any other groups, with a mean shoot length of  $27.84 \pm 8.00$  mm. The results indicate that shoot length was notably inhibited at certain concentrations, namely 5 ppm and 1000 ppm. This disparity may be attributed to outliers within the data from the 5-ppm group, potentially skewing the results. Additionally, it's plausible that the increment of CuO NPs could lead to an inhibitory effect on shoot growth beyond the concentration of 100 ppm, suggesting a potential threshold for CuO NPs beyond which their adverse impact on shoot development becomes more pronounced. Previous studies have yielded similar results regarding the inhibition of shoot length at high concentrations of CuO NPs. For instance, in a study on the foliar application of copper oxide nanoparticles in *Brassica juncea*, concentrations ranging from 0 to 16 mg/L were investigated. It was observed that at 8 mg/L, the shoot length was induced and reached its maximum. However, at 16 mg/L, the shoot length decreased, indicating that concentrations higher than the optimum level could adversely affect shoot length (Faraz *et al.*, 2022). Similar outcomes were observed in a study involving the treatment of tomato seeds with green-synthesized CuO NPs across a range of concentrations from 0 to 4000 µg/ml specifically, the shoot length was induced at a concentration of 4 µg/mL. However, subsequent increases in CuO NPs concentration led to a decrease in shoot length, indicating an adverse effect on shoot growth with higher concentrations (Khalidari *et al.*, 2021). These findings imply the biphasic effect of nanoparticles, wherein low concentrations stimulate or enhance a biological process, but after reaching an optimum concentration, inhibition or toxicity affects the seedlings. Further studies are required to understand this

non-linear relationship for each nanoparticle with each plant.

Figure 11 illustrates the seed vigor index of tomato under different CuO NPs concentrations. Seed vigor assesses the potential for seed germination and subsequent growth. The index combines parameters of germination rate and seedling growth to provide a comprehensive evaluation of seed vigor. High seed vigor index values indicate seeds that are more likely to germinate quickly and produce vigorous, healthy seedlings. In the current study, the data were analyzed using one-way ANOVA and found to be significant within a confidence interval of 0.0001 ( $F = 7.553$ ). In Dunnett's test, the significant difference between 0 and 1000 ppm suggests the inhibitory effect of CuO NPs on the seed vigor index for tomatoes. According to the DMRT test, the treatment group with the highest mean, 50 ppm, had a mean seed vigor index of  $3373.56 \pm 1303.54$ . Treatment groups of 0, 5, 10, and 100 ppm showed no significance within the group but exhibited significant differences compared to 50 ppm and 1000 ppm, with mean seed vigor indices of  $3176.000 \pm 1720.04$ ,  $3069.41 \pm 2355.8508$ ,  $3192 \pm 1345.10$ , and  $3182 \pm 866.94$ , respectively. The treatment group of 500 ppm showed no significant difference compared to the 50 ppm group, with a mean seed vigor index of  $2280 \pm 719.46$ . The current research clearly found that the green-synthesized CuO NPs produced by *M. pigra* had an adverse inhibitory effect on tomato seedling seed vigor at the concentration of 1000 ppm while showing an inducing effect at the concentration of 50 ppm. In a previous study, copper oxide nanoparticles derived from *Zizyphus spina* leaf extract were investigated regarding their effects on tomato seeds. It was found that the maximum seed vigor index was observed at concentrations of 100 and 250 ppm (El-Abeid *et al.*, 2024). A study on CuO nanoparticles' effects on wheat confirmed similar results, indicating that beyond the 1 ppm to 10 ppm treatment range, a drastic decline in seed vigor index was observed (Ibrahim *et al.*, 2022). In the study on the biosynthesis of Zinc Oxide Nanoparticles via Leaf Extracts of *Catharanthus roseus* on Seedling Vigor of *Eleusine coracana*, they were treated with different Zinc Oxide Nanoparticles concentrations ranging from 0, 100, 500, to 1000 ppm. It was observed that the maximum seed vigor index was achieved at 100 and 500 ppm, while the lowest seed vigor index was recorded at 1000 ppm, indicating the inhibitory effect of high concentrations of nanoparticles (Mishra *et al.*, 2023). In a previous study on ZnO-NPs conducted on *Camelina* seedlings, it was found that the highest seed vigor index was observed at 1 ppm, with a decline in seed vigor index beyond this concentration. The minimum seed vigor index was recorded at 1000 ppm (Sarkhosh *et al.*, 2022). The results obtained aligning with previous studies suggest a significant inhibitory effect of CuO nanoparticles synthesized via green synthesis using *M. pigra* on tomato seedlings, particularly at higher concentrations.

## CONCLUSION

In conclusion, this study successfully synthesized copper oxide nanoparticles (CuO NPs) using *Mimosa pigra* leaf extract, with UV-visible spectroscopy, SEM, XRD, and FTIR analysis confirming their synthesis and providing detailed structural insights. The UV-visible spectrum showed a surface plasmon resonance (SPR) peak at 224 nm, while SEM revealed a nanoscale morphology with an average size of 108 nm. XRD analysis confirmed a crystalline monoclinic structure with an average crystallite size of 30.68 nm, and FTIR spectra highlighted key functional groups, including Cu-O bond vibrations and plant-related compounds. Our investigations revealed a significant inhibitory effect on root growth and seed vigor at CuO NP concentrations greater than 50 ppm. We observed a biphasic effect of these nanoparticles on various aspects of tomato seedling growth and vigor, including germination rate, fresh weight of seedlings, root length, shoot length, and seed vigor index. This biphasic response underscores the complex nature of nanoparticle-plant interactions, where low concentrations may stimulate growth, while higher concentrations result in inhibition or toxicity. This non-linear relationship highlights the need to optimize nanoparticle concentrations to achieve desired outcomes in agricultural applications. Additionally, our study contributes to the growing body of research on nanoparticle exposure's impact on plant health and emphasizes the need for further investigation into the underlying mechanisms. Based on our findings, we recommend further studies within the concentration range of 50 ppm to 100 ppm.

## REFERENCES

- Acharya, P., Jayaprakasha, G. K., Crosby, K. M., Jifon, J. L., & Patil, B. S. (2019). Green-synthesized nanoparticles enhanced seedling growth, yield, and quality of onion (*Allium cepa* L.). *ACS Sustainable Chemistry & Engineering*, 7(17), 14580–14590. <https://doi.org/10.1021/acssuschemeng.9b02180>
- Ahmad, T., Irfan, M., Bustam, M. A., & Bhattacharjee, S. (2016). Effect of reaction time on green synthesis of gold nanoparticles by using aqueous extract of *Elaeis guineensis* (oil palm leaves). *Procedia Engineering*, 148, 467–472. <https://doi.org/10.1016/j.proeng.2016.06.465>
- Ahuchaogu, A. A., Chukwu, O. J., & Echeme, J. O. (2017). Secondary metabolites from *Mimosa pudica*: Isolation, purification, and NMR characterization. *IOSR Journal of Applied Chemistry*, 10(3), 15–20. <https://doi.org/10.9790/5736-1003011520>
- Alhalili, Z. (2022). Green synthesis of copper oxide nanoparticles (CuO NPs) from *Eucalyptus globulus* leaf extract: Adsorption and design of experiments. *Arabian Journal of Chemistry*, 15(5), 103739. <https://doi.org/10.1016/j.arabjc.2022.103739>
- Alloway, B. J. (2014). *Heavy metals in soils: Trace metals and metalloids in soils and their bioavailability*. Springer Verlag.
- Altemimi, A., Lakhssassi, N., Baharlouei, A., Watson, D., & Lightfoot, D. (2017). Phytochemicals: Extraction, isolation, and identification of bioactive compounds from plant extracts. *Plants*, 6(4), 42. <https://doi.org/10.3390/plants6040042>
- Amaliyah, S., Pangesti, D. P., Masruri, M., Sabarudin, A., & Sumitro, S. B. (2020). Green synthesis and characterization of copper nanoparticles using *Piper retrofractum* Vahl extract as bioreductor and capping agent. *Heliyon*, 6(8), e04636. <https://doi.org/10.1016/j.heliyon.2020.e04636>
- Amin, F., Fozia, Khattak, B., Alotaibi, A., Qasim, M., Ahmad, I., Ullah, R., Bourhia, M., Gul, A., Zahoor, S., & Ahmad, R. (2021). Green synthesis of copper oxide nanoparticles using *Aerva javanica* leaf extract and their characterization and investigation of in vitro antimicrobial potential and cytotoxic activities. *Evidence-Based Complementary and Alternative Medicine*, 2021, 1–12. <https://doi.org/10.1155/2021/5589703>
- Amirmoradi, S., & Feizi, H. (2017). Can mean germination time predict seed vigor of canola (*Brassica napus* L.) seed lots? *Acta Agrobotanica*, 70(4). <https://doi.org/10.5586/aa.1729>
- Ansari, M., Ahmed, S., Abbasi, A., Muhammad Tajammal Khan, Subhan, M., Bukhari, N. A., Ashraf Atef Hatamleh, & Abdelsalam, N. R. (2023). Plant-mediated fabrication of silver nanoparticles, process optimization, and impact on tomato plant. *Scientific Reports*, 13(1). <https://doi.org/10.1038/s41598-023-45038-x>
- Atha, D. H., Wang, H.-Q., Petersen, E. J., Cleveland, D., Holbrook, R. D., Jaruga, P., Dizdaroglu, M., Xing, B., & Nelson, B. C. (2012). Copper oxide nanoparticle mediated DNA damage in terrestrial plant models. *Environmental Science & Technology*, 46(3), 1819–1827. <https://doi.org/10.1021/es202660k>
- Azhar, W., Ali Raza Khan, Salam, A., Zaid Ulhassan, Qi, J., Shah, G., Liu, Y., Chunyan, Y., Yang, S., & Gan, Y. (2022). Ethylene accelerates copper oxide nanoparticle-induced toxicity at physiological, biochemical, and ultrastructural levels in rice seedlings. *Environmental Science and Pollution Research*, 30(10), 26137–26149. <https://doi.org/10.1007/s11356-022-23915-8>
- Banu, K. S. (2015). General techniques involved in phytochemical analysis. *International Journal of Advanced Research in Chemical Science*, 2(4), 25–32.
- Černík, M., & Thekkae Padil, V. V. (2013). Green synthesis of copper oxide nanoparticles using gum karaya as a biotemplate and their antibacterial application. *International Journal of Nanomedicine*, 8, 89. <https://doi.org/10.2147/ijn.s40599>
- Chung, I. M., Rekha, K., Venkidasamy, B., & Thiruvengadam, M. (2019). Effect of copper oxide nanoparticles on the physiology, bioactive molecules, and transcriptional changes in *Brassica rapa* ssp. *rapa* seedlings. *Water, Air, & Soil Pollution*, 230(2). <https://doi.org/10.1007/s11270-019-4084-2>
- Dawood, M. G. (2018). Stimulating plant tolerance against

- abiotic stress through seed priming. In *Seed priming: The essential role of water in plant seed biology* (pp. 147–183). [https://doi.org/10.1007/978-981-13-0032-5\\_10](https://doi.org/10.1007/978-981-13-0032-5_10)
- Dev, A., Srivastava, A. K., & Karmakar, S. (2017). Nanomaterial toxicity for plants. *Environmental Chemistry Letters*, 16(1), 85–100. <https://doi.org/10.1007/s10311-017-0667-6>
- Dimkpa, C. O., McLean, J. E., Latta, D. E., Manangón, E., Britt, D. W., Johnson, W. P., Boyanov, M. I., & Anderson, A. J. (2012). CuO and ZnO nanoparticles: Phytotoxicity, metal speciation, and induction of oxidative stress in sand-grown wheat. *Journal of Nanoparticle Research*, 14(9). <https://doi.org/10.1007/s11051-012-1125-9>
- El-Abeid, S. E., Mosa, M. A., Mohamed, S., Saleh, A. M., El-Khateeb, M. A., & Maha. (2024). Antifungal activity of copper oxide nanoparticles derived from *Zizyphus spina* leaf extract against Fusarium root rot disease in tomato plants. *Journal of Nanobiotechnology*, 22(1). <https://doi.org/10.1186/s12951-023-02281-8>
- Elamin, N. Y., & Taha, A. (2023). Biogenic synthesis of copper oxide nanoparticles using Pimpinella anisum seed extract: Characterization and antibacterial activity. *Oriental Journal of Chemistry*, 39(1), 69–74. <https://doi.org/10.13005/ojc/390108>
- Faraz, A., Faizan, M., Hayat, S., & Alam, P. (2022). Foliar application of copper oxide nanoparticles increases the photosynthetic efficiency and antioxidant activity in Brassica juncea. *Journal of Food Quality*, 2022, 1–10. <https://doi.org/10.1155/2022/5535100>
- Faraz, A., Faizan, M., Rajput, V. D., Minkina, T., Hayat, S., Faisal, M., Alatar, A. A., & Abdel-Salam, E. M. (2023). CuO nanoparticle-mediated seed priming improves physio-biochemical and enzymatic activities of Brassica juncea. *Plants*, 12(4), 803. <https://doi.org/10.3390/plants12040803>
- Feigl, G. (2023). The impact of copper oxide nanoparticles on plant growth: A comprehensive review. *Journal of Plant Interactions*, 18(1). <https://doi.org/10.1080/17429145.2023.2243098>
- Garcia, D., Zhao, S., Arif, S., Zhao, Y., Ming, L., & Huang, D. (2022). Seed priming technology as a key strategy to increase crop plant production under adverse environmental conditions. <https://doi.org/10.33140/jahr.05.01.04>
- Gross, M. S., Bean, T. G., Hladik, M. L., Rattner, B. A., & Kuivila, K. M. (2020). Uptake, metabolism, and elimination of fungicides from coated wheat seeds in Japanese quail (*Coturnix japonica*). *Journal of Agricultural and Food Chemistry*, 68(6), 1514–1524. <https://doi.org/10.1021/acs.jafc.9b05668>
- Hosseinzadeh, E., Foroumadi, A., & Firoozpour, L. (2023). What is the role of phytochemical compounds as capping agents for the inhibition of aggregation in the green synthesis of metal oxide nanoparticles? A DFT molecular level response. *Inorganic Chemistry Communications*, 147, 110243. <https://doi.org/10.1016/j.inoche.2022.110243>
- Ibrahim, A. S., Ali, G. A. M., Hassanein, A., Attia, A. M., & Marzouk, E. R. (2022). Toxicity and uptake of CuO nanoparticles: Evaluation of an emerging nanofertilizer on wheat (*Triticum aestivum* L.) plant. *Sustainability*, 14(9), 4914. <https://doi.org/10.3390/su14094914>
- Kacziba, B., Szierer, Á., Mészáros, E., Rónavári, A., Kónya, Z., & Feigl, G. (2023). Exploration of the homeostasis of signaling molecules in monocotyledonous crops with different CuO nanoparticle tolerance. *Plant Stress*, 7, 100145. <https://doi.org/10.1016/j.stress.2023.100145>
- Kadri, O., Karmous, I., Kharbech, O., Arfaoui, H., & Chaoui, A. (2022). Cu and CuO nanoparticles affected the germination and the growth of barley (*Hordeum vulgare* L.) seedling. *Bulletin of Environmental Contamination and Toxicology*, 108(3), 585–593. <https://doi.org/10.1007/s00128-021-03425-y>
- Karami Mehrian, S., & de Lima, R. (2016). Nanoparticles cyto- and genotoxicity in plants: Mechanisms and abnormalities. *Environmental Nanotechnology, Monitoring & Management*, 6, 184–193. <https://doi.org/10.1016/j.enmm.2016.08.003>
- Karunagaran, V., & Sen, S. (2011). Biosynthesis of nanoparticles. *International Journal of Pharmaceutical Sciences and Research*, 2, 2781–2785.
- Khaldari, I., Naghavi, M. R., & Motamedi, E. (2021). Synthesis of green and pure copper oxide nanoparticles using two plant resources via solid-state route and their phytotoxicity assessment. *RSC Advances*, 11(6), 3346–3353. <https://doi.org/10.1039/d0ra09924d>
- Khodakovskaya, M. V., de Silva, K., Biris, A. S., Dervishi, E., & Villagarcia, H. (2012). Carbon nanotubes induce growth enhancement of tobacco cells. *ACS Nano*, 6(3), 2128–2135. <https://doi.org/10.1021/nn204643g>
- Kuppusamy, P., Yusoff, M. M., Maniam, G. P., & Govindan, N. (2016). Biosynthesis of metallic nanoparticles using plant derivatives and their new avenues in pharmacological applications – An updated report. *Saudi Pharmaceutical Journal*, 24(4), 473–484. <https://doi.org/10.1016/j.jsps.2014.11.013>
- Kumar, C. G., Pombala, S., Poornachandra, Y., & Agarwal, S. V. (2016). Synthesis, characterization, and applications of nanobiomaterials for antimicrobial therapy. In *Nanobiomaterials in antimicrobial therapy* (pp. 103–152). <https://doi.org/10.1016/b978-0-323-42864-4.00004-x>
- Lade, B., & Shanware, A. (2020). Phytonanofabrication: Methodology and factors affecting biosynthesis of nanoparticles. <https://doi.org/10.5772/intechopen.90918>
- Li, K. E., Chang, Z. Y., Shen, C. X., & Yao, N. (2015). Toxicity of nanomaterials to plants. In *Nanomaterials and plants* (pp. 101–123). [https://doi.org/10.1007/978-3-319-14502-0\\_6](https://doi.org/10.1007/978-3-319-14502-0_6)
- Mahmoud, A. E. D., Al-Qahtani, K. M., Alflajj, S. O., Al-Qahtani, S. F., & Alsamhan, F. A. (2021). Green

- copper oxide nanoparticles for lead, nickel, and cadmium removal from contaminated water. *Scientific Reports*, 11(1). <https://doi.org/10.1038/s41598-021-91093-7>
- Maisuria, K., & Patel, S. T. (2009). Seed germinability, root and shoot length and vigour index of soybean as influenced by rhizosphere fungi. *Karnataka Journal of Agricultural Sciences*, 22, 1120–1122. <https://api.semanticscholar.org/corpusid:82624279>
- Margenot, A. J., Rippner, D. A., Dumlao, M. R., Nezami, S., Green, P. G., Parikh, S. J., & McElrone, A. J. (2018). Copper oxide nanoparticle effects on root growth and hydraulic conductivity of two vegetable crops. *Plant and Soil*, 431(1-2), 333–345. <https://doi.org/10.1007/s11104-018-3741-3>
- Martins, L. L., & Mourato, M. P. (2006). Effect of excess copper on tomato plants: Growth parameters, enzyme activities, chlorophyll, and mineral content. *Journal of Plant Nutrition*, 29(12), 2179–2198. <https://doi.org/10.1080/01904160600972845>
- Mhara, Y., Sakhraoui, A., Ferchichi, Y., Khamassi, K., & Slim, R. (2022). The germination and early seedling growth of three *Tunisian Lupinus L.* species under copper and zinc-induced stress. 31, 11514–11521.
- Mishra, D., Chitara, M. K., Negi, S., Singh, J. P., Kumar, R., & Chaturvedi, P. (2023). Biosynthesis of zinc oxide nanoparticles via leaf extracts of *Catharanthus roseus* (L.) G. Don and their application in improving seed germination potential and seedling vigor of *Eleusine coracana* (L.) Gaertn. *Advances in Agriculture*, 2023, 1–11. <https://doi.org/10.1155/2023/7412714>
- Montanha, G. S., Santos, E., Paulo, J., de Almeida, E., Colzato, M., & Pereira, W. (2020). Zinc nanocoated seeds: An alternative to boost soybean seed germination and seedling development. *SN Applied Sciences*, 2(5). <https://doi.org/10.1007/s42452-020-2630-6>
- Munns, R. (2002). Comparative physiology of salt and water stress. *Plant, Cell & Environment*, 25(2), 239–250. <https://doi.org/10.1046/j.0016-8025.2001.00808.x>
- Munns, R., & Tester, M. (2008). Mechanisms of salinity tolerance. *Annual Review of Plant Biology*, 59(1), 651–681. <https://doi.org/10.1146/annurev.arplant.59.032607.092911>
- Murali, M., Gowtham, H. G., Singh, S. B., Shilpa, N., Aiyaz, M., Alomary, M. N., Alshamrani, M., Salawi, A., Almoshari, Y., Ansari, M. A., & Amruthesh, K. N. (2022). Fate, bioaccumulation and toxicity of engineered nanomaterials in plants: Current challenges and future prospects. *Science of the Total Environment*, 811, 152249. <https://doi.org/10.1016/j.scitotenv.2021.152249>
- Naz, S., Gul, A., & Zia, M. (2020). Toxicity of copper oxide nanoparticles: A review study. *IET Nanobiotechnology*, 14(1), 1–13. <https://doi.org/10.1049/iet-nbt.2019.0176>
- Olusayo, S., Nnamdi, E., Afieroho, O., & Shorinwa, O. (2016). Evaluation of *Mimosa pigra* roots on haematological and biochemical parameters of albino rats. *World Journal of Pharmaceutical Research*, 5, 810–822. <https://doi.org/10.20959/wjpr201645843>
- Panyuta, O., Belava, V. N., Fomaidi, S., Kalinichenko, O., Volkogon, M., & Taran, N. (2016). The effect of pre-sowing seed treatment with metal nanoparticles on the formation of the defensive reaction of wheat seedlings infected with the eyespot causal agent. *Journal of Nanomaterials*, 11(1). <https://doi.org/10.1186/s11671-016-1305-0>
- Rangasamy, M., Kumar Gopal, S., Indhumathi, A., Loganathan, S., Manikandan, S., & Naresh, R. (2023). Green synthesis and characterization of copper oxide nanoparticles using *Tecoma stans*. *Journal of Pharmaceutical Research International*, 35(7), 9–16. <https://doi.org/10.9734/jpri/2023/v35i77335>
- Redhi, G. G. (2018). Green synthesis of metal nanoparticles and its reaction mechanisms. In *Green synthesis of nanoparticles* (pp. 113–139). <https://doi.org/10.1002/9781119418900.ch4>
- Rosado-Vallado, M., Brito-Loeza, W., Mena-Rejón, G. J., Quintero-Marmol, E., & Flores-Guido, J. S. (2000). Antimicrobial activity of Fabaceae species used in Yucatán traditional medicine. *Fitoterapia*, 71(5), 570–573. [https://doi.org/10.1016/s0367-326x\(00\)00200-8](https://doi.org/10.1016/s0367-326x(00)00200-8)
- Sabouri, Z., Sabouri, M., Amiri, M. S., Khatami, M., & Darroudi, M. (2020). Plant-based synthesis of cerium oxide nanoparticles using *Rheum turkestanicum* extract and evaluation of their cytotoxicity and photocatalytic properties. *Materials Technology*, 1–14. <https://doi.org/10.1080/10667857.2020.1863573>
- Sabouri, Z., Sabouri, S., Sadat, S., Mostafapour, A., Gheibihayat, S. M., & Darroudi, M. (2022). Plant-based synthesis of Ag-doped ZnO/MgO nanocomposites using *Caccinia macranthera* extract and evaluation of their photocatalytic activity, cytotoxicity, and potential application as a novel sensor for detection of Pb<sup>2+</sup> ions. *Biomass Conversion and Biorefinery*. <https://doi.org/10.1007/s13399-022-02907-1>
- Seifipour, R., Nozari, M., & Pishkar, L. (2020). Green synthesis of silver nanoparticles using *Tragopogon collinus* leaf extract and study of their antibacterial effects. *Journal of Inorganic and Organometallic Polymers and Materials*. <https://doi.org/10.1007/s10904-020-01441-9>
- Shabbir, Z., Sardar, A., Shabbir, A., Abbas, G., Shamshad, S., Khalid, S., Natasha, M., Murtaza, G., Dumat, C., & Shahid, M. (2020). Copper uptake, essentiality, toxicity, detoxification, and risk assessment in soil-plant environment. *Chemosphere*, 259, 127436. <https://doi.org/10.1016/j.chemosphere.2020.127436>
- Shalaby, T. A., Bayoumi, Y., Abdalla, N., Taha, H., Alshaal, T., Shehata, S., Amer, M., Domokos-Szabolcsy, É., & El-Ramady, H. (2016). Nanoparticles, soils, plants and sustainable agriculture. In *Nanoscience in Food and Agriculture 1* (pp. 283–312). [https://doi.org/10.1007/978-3-319-39303-2\\_10](https://doi.org/10.1007/978-3-319-39303-2_10)

- Shaw, A. K., & Hossain, Z. (2013). Impact of nano-CuO stress on rice (*Oryza sativa* L.) seedlings. *Chemosphere*, 93(6), 906–915. <https://doi.org/10.1016/j.chemosphere.2013.05.044>
- Shende, S., Ingle, A. P., Gade, A., & Rai, M. (2015). Green synthesis of copper nanoparticles by Citrus medica Linn. (Idilimbu) juice and its antimicrobial activity. *World Journal of Microbiology and Biotechnology*, 31(6), 865–873. <https://doi.org/10.1007/s11274-015-1840-3>
- Shkir, M. (2022). Green method for synthesis and characterization of copper oxide nanoparticles using mulberry plant extract and their antibacterial, antioxidant, and photocatalytic activity. *Physica Scripta*, 97(10), 105001. <https://doi.org/10.1088/1402-4896/ac8a7a>
- Siddiqi, K. S., & Husen, A. (2020). Current status of plant metabolite-based fabrication of copper/copper oxide nanoparticles and their applications: A review. *Biomaterials Research*, 24(1). <https://doi.org/10.1186/s40824-020-00188-1>
- Singh, A., B L R, Madhavi, & Sagar, N. (2021). An overview of green synthesis mediated metal nanoparticles preparation and its scale-up opportunities. *Journal of Drug Delivery and Therapeutics*, 11, 304–314. <https://doi.org/10.22270/jddt.v11i6.5082>
- Sravanthi, M., Kumar, D. Muni, Usha, B., Rao, M. Mahendra, Hemalatha, K. P. J., & Ravichandra, M. (2016). Biological synthesis and characterization of copper oxide nanoparticles using Antigonon leptopus leaf extract and their antibacterial activity. *International Journal of Advanced Research*, 4(8), 589–602. <https://doi.org/10.21474/ijar01/1251>
- Vijayaraghavan, K., & Ashokkumar, T. (2017). Plant-mediated biosynthesis of metallic nanoparticles: A review of literature, factors affecting synthesis, characterization techniques, and applications. *Journal of Environmental Chemical Engineering*, 5(5), 4866–4883. <https://doi.org/10.1016/j.jece.2017.09.026>
- Wang, X., Xie, H., Wang, P., & Yin, H. (2023). Nanoparticles in plants: Uptake, transport, and physiological activity in leaf and root. *Materials*, 16(8), 3097. <https://doi.org/10.3390/ma16083097>
- Yang, Z., Xiao, Y., Jiao, T., Zhang, Y., Chen, J., & Gao, Y. (2020). Effects of copper oxide nanoparticles on the growth of rice (*Oryza sativa* L.) seedlings and the relevant physiological responses. *International Journal of Environmental Research and Public Health*, 17(4), 1260. <https://doi.org/10.3390/ijerph17041260>
- Zhang, D., Hua, T., Xiao, F., Chen, C., Gersberg, R. M., Liu, Y., Ng, W. J., & Tan, S. K. (2014). Uptake and accumulation of CuO nanoparticles and CdS/ZnS quantum dot nanoparticles by *Schoenoplectus tabernaemontani* in hydroponic mesocosms. *Ecological Engineering*, 70, 114–123. <https://doi.org/10.1016/j.ecoleng.2014.04.018>
- Zhang, D., Liu, X., Ma, J., Yang, H., Zhang, W., & Li, C. (2019). Genotypic differences and glutathione metabolism response in wheat exposed to copper. *Environmental and Experimental Botany*, 157, 250–259. <https://doi.org/10.1016/j.envexpbot.2018.06.032>
- Zheng, L., Hong, F., Lu, S., & Liu, C. (2005). Effect of nano-TiO<sub>2</sub> on strength of naturally aged seeds and growth of spinach. *Biological Trace Element Research*, 104(1), 83–92. <https://doi.org/10.1385/bter:104:1:083>